Supporting Information

Le Scouarnec *et al.* 10.1073/pnas.0805500105

SI Methods

Clinical Investigation. The study was conducted according to the French guidelines for genetic research and was approved by the ethical committee of Nantes University Hospital. Informed written consent was obtained from each family member who agreed to participate in the study and blood samples were collected for genetic analysis. Clinical investigation included a review of medical history, a physical examination, a 12-lead ECG, and an echocardiography. Diagnosis was established independently by two clinicians, and heart rate, QT, and QTU durations were measured at rest on the first recorded ECG when available. QTc were calculated by using Bazett's formula. QTU was measured at the end of the U wave in patients presenting a sinusoidal aspect of the repolarization. SND was defined by (*i*) a heart rate under 50 bpm at rest in adults or a lower than expected heart rate for the age in children or (*ii*) by an abnormal rhythm (junctional escape or coronary sinus rhythm). The clinical status of the family members was defined as affected whether they were affected by either SND or AF or an abnormal ventricular repolarization with a prominent U wave.

Genetic Analysis. Family 1 genetic analysis has been previously published (1). For family 2, DNA was isolated from peripheral blood lymphocytes with standard methods. All family members included in the study were genotyped and sequenced by using a 3730 DNA Analyzer (Applied Biosystems). Mutation analysis was conducted by direct sequencing of the *ANK2* gene. All 46 exons of the *AnkB* gene were amplified by using intronic primers (1). We carried out two-point linkage analysis with the SUPERLINK program in the easyLINKAGE software package. For linkage calculations, we assumed dominant inheritance with a disease–allele frequency of 0.01% and penetrance was set at 90%.

Lentiviral Expression. We subcloned 220-kDa AnkB-GFP by PCR into the lentiviral shuttle vector pCDH1-MCS1/2 (System Biosciences) by using the restriction sites NheI and SwaI. PCR-based site-directed mutagenesis was performed to change residue 1425 from glutamic acid to glycine. Two 10-cm plates of HEK293TN cells and 10 μg of WT or E1425G AnkB-GFP were transfected with pPACKH1 lentivector packaging kit (System Bioscience) overnight by using Effectene (Qiagen). The cells were maintained in a minimal volume of DMEM/2% FCS for another 48 h. The media was drawn off and concentrated by centrifugation by using Centriplus columns (Millipore) for 3 h at 4°C. Relative transduction efficiencies were evaluated by GFP expression in HEK293 cells following a 24-h period of infection.

Antibodies. Primary antibodies used for experiments included affinity-purified AnkB (monoclonal and polyclonal), ankyrin-G (polyclonal), and GFP (polyclonal) I_g. Rabbit anti-$Ca_v1.2$, rabbit anti-$Ca_v1.3$, rabbit anti-$Ca_v3.1$, and rabbit anti-HCN4 were purchased from Alomone Labs. Rabbit anti-IP_3R, mouse anti-NKA $\alpha1$, mouse anti-NKA $\beta1$, and mouse anti-RyR_2 were purchased from Affinity BioReagents. Rabbit anti-NCX1 was purchased from Swant, mouse anti-NCX1 was purchased from Fitzgerald Industries, mouse anti-neurofilament was purchased from the Developmental Studies Hybridoma Bank, and rabbit anti-NKA $\alpha2/3$ was purchased from Millipore. Gap junction protein antibodies included rabbit anti-connexin 40 (Chemicon), rabbit anti-connexin 43 (Zymed), mouse anti-connexin 43 (Chemicon), and rabbit anti-connexin 45 (Zymed). Secondary antibodies included goat anti-rabbit and goat anti-mouse Alexa Fluor 488 and 568 (Molecular Probes).

Immunoblots. Equal quantities of protein lysate obtained from $AnkB^{+/-}$ and WT heart tissues (pooled from multiple mouse hearts/genotype) or human heart tissues were analyzed by SDS/PAGE (3–8% Tris-acetate gels) and immunoblotted following protocols as previously described (1). Parallel immunoblots were performed by using an unrelated protein antibody (NHERF1, Sigma) to demonstrate equal protein loading. Blots were developed by using HRP-conjugated donkey anti-rabbit and donkey anti-mouse secondary antibodies (Jackson ImmunoReagents) and ECL (Pierce).

Immunofluorescence. Freshly isolated or cultured sinoatrial cells were washed with PBS (PBS, pH 7.4) and fixed in 2% paraformaldehyde. Cells were blocked/permeabilized in PBS containing 0.075% Triton X-100, 2 mg/ml BSA, and 3% fish gelatin and incubated in primary antibody overnight at 4°C. Following PBS washes, cells were incubated in secondary antibody (Alexa 488, 568; 633; Molecular Probes) for 2 h at room temperature and mounted by using Vectashield (Vector) and #1 coverslips. Images were collected on Zeiss 510 Meta confocal microscope (10× power, 0.3 NA; 20× power, 0.8 NA; 40× power oil, 1.3 NA; and 63 power oil, 1.40 NA (Zeiss); pinhole equals 1.0 Airy Disk) by using Carl Zeiss Imaging software. Images were imported into Adobe Photoshop for cropping and linear contrast adjustment. SAN Preparation for Ca^{2+} Imaging and Biochemistry.

Mice were anesthetized and a dissecting microscope was used to remove each heart, and each heart was pinned to a clay surface to excise the right atrium. This investigation conforms to the Guide for the Care and Use of Laboratory Animals published by the National Institutes of Health (Pub. No. 85-23, 1996) and protocols used in the study were approved by the University of Iowa Institutional Animal Care and Use Committee. For isolation of SAN tissue from both mouse and human heart, the SAN region limited by the crista terminalis, atrial septum, and orifice of superior vena cava was dissected as described by DiFrancesco (2), and Mangoni and Nargeot (3). The preparation was trimmed, leaving only the SAN region. For Ca^{2+} imaging of mouse SAN cells, the SAN preparation was loaded with the membrane-permeant fluorescent Ca^{2+} indicator, Fluo-3 AM (10 μmol/L), in Tyrode solution for 30 min. Fluorescent signals, excited by the 488-nm line of Argon laser, were recorded in line-scan mode (1.93 ms per line) by using a Zeiss LSM 510 Meta confocal microscope. The power spectrum analysis of Ca^{2+} transients were performed by using pClamp 10 software. For biochemistry experiments, whole SAN preparations were flash frozen for subsequent processing. The dissected human SAN region was cut into multiple tissue pieces. Each piece was flash frozen, and the central SAN region was confirmed by immunoblot for positive (HCN4) and negative (Cx43) antibody markers. Human right atrial tissue was obtained from healthy donor hearts that were not suitable for transplantation (subclinical atherosclerosis, old age, no matching recipients) through the Iowa Donors Network and through the National Disease Research Interchange, Inc. The investigation conforms with the principles outlined in the Declaration of Helsinki (4). Age and sex were the only identifying information acquired from the tissue providers, and the University of Iowa Human Subjects Committee deemed that informed consent from each patient

was not required. None of the patients died from cardiac-related causes.

RNA Preparation and TaqMan Quantitative RT-PCR. RNA preparation and TaqMan Low Density Arrays were performed as described previously (see details in supporting information (SI) *Methods*, ref 5).

SAN Preparation and Electrophysiological Recordings. SAN pacemaker cells were isolated from age- and sex-matched WT or AnkB$^{+/-}$ C57BL/6 adult mice donors of either sex as described (3). Briefly, beating hearts were removed following i.p. injection of 2.5% Avertin solution. The SAN region (bordered by crista terminalis, interatrial septum, superior and inferior vena cava) was excised in prewarmed (35°C) Tyrode solution (containing in mM: NaCl, 140; Hepes, 5; glucose, 5.5; KCl, 5.4; $CaCl_2$, 1.8; $MgCl_2$, 1). SAN tissue strips were then transferred to prewarmed calcium-free Tyrode solution and cut into ≈10 small pieces. These SAN pieces were transferred to prewarmed digestion solution (containing in mM: NaCl, 140; Hepes, 5; glucose, 5.5; KCl, 5.4; $CaCl_2$, 0.2; $MgCl_2$, 0.5; KH_2PO_4, 1.2; taurine, 50; BSA, 1 mg/ml; collagenase, 229 units/ml; elastase, 1.9 units/ml; protease, 0.9 units/ml) and incubated for approximately 35 min in a 35°C water bath with manual agitation every 5 min. The digestion solution was replaced with prewarmed KB solution (containing in mM: Glutamic acid K, 100; Hepes, 5; glucose, 20; KCl, 25; K aspartate, 10; $MgSO_4$, 2; KH_2PO_4, 10; taurine, 20; creatine, 5; EGTA, 0.5; BSA, 1 mg/ml) and gently triturated by using a pipette with an inner diameter of 3 mm. The SAN myocytes were readapted to normal, extracellular Ca^{2+} concentration by the addition of a solution containing NaCl (10 mM) and $CaCl_2$ (1.8 mM) followed by Tyrode's solution with BSA (1 mg/ml). The SAN myocytes were then kept in storage solution (containing in mM: NaCl, 100; glutamic acid K, 14; KCl, 35; $CaCl_2$, 1.3; $MgCl_2$, 0.7; KH_2PO_4, 2; taurine, 2; BSA, 1 mg/ml) until used for electrophysiology experiments. For I_{NCX} recording, we used a standard protocol (6). Whole-cell recordings were obtained at RT with the use of standard patch-clamp techniques. Membrane current was assessed by use of an Axopatch-200B amplifier and a CV-203BU head stage (Axon Instruments). Experimental monitoring, data acquisition, and data analysis were accomplished with the use of the software package PClamp 8.0 with the Digidata 1320A acquisition system (Axon Instruments). Patch pipettes were pulled from thin-walled glass capillary tubes and heat polished. The electrode resistance ranged from 2–4 MΩ. The external solution contained the following (in mmol/L): NaCl, 145; $MgCl_2$, 1; Hepes, 5; $CaCl_2$, 2; CsCl, 5; and glucose, 10 (pH 7.4, adjusted with NaOH). The internal solution contained the following (in mmol/L): CsCl, 65; NaCl, 20; Na_2ATP, 5; $CaCl_2$, 6; $MgCl_2$, 4; Hepes, 10; tetraethyl ammonium chloride, 20; and EGTA, 21 (pH 7.2, adjusted with CsOH). Membrane currents were elicited with the use of standard voltage ramp protocol. From a holding potential of −40 mV, a 100-ms step depolarization to +50 mV was followed by a descending voltage ramp (from +50 mV to −100 mV at 100 mV/s). The protocol was applied every 12 seconds. I_{NCX} was measured as the Ni-sensitive current. Ni^{2+} (5 mmol/L) was added to define the fraction of current that derives from NCX (the difference between total current and post-Ni^{2+} current). Membrane capacitance was read directly from the membrane test of PClamp 8.0 before compensating for series resistance and membrane capacitance. For calcium current recordings, electrophysiological recordings were acquired at room temperature, by using an Axopatch 200A patch-clamp amplifier (Axon Instruments). Electrodes were fashioned from borosilicate glass capillaries (World Precision Instruments, B150-F4) and were filled with an internal solution containing (mM): cesium methane sulfonate (Cs-$MeSO_3$), 150; CsCl, 5; Hepes, 10; EGTA, 10; MgCl2, 1; and MgATP, 4 (pH 7.2, adjusted with CsOH). Typically, pipettes had resistances of 3–4 M148, before series resistance compensation of 60–75%. For formation of gigaohm seals and initial break-in to the whole-cell voltage clamp configuration, cells were perfused with normal Tyrode solution containing (mM): NaCl, 138; KCl, 4; $CaCl_2$, 2; $MgCl_2$, 1; NaH_2PO_4, 0.33; Hepes, 10; and glucose, 10 (pH 7.4, adjusted with NaOH). Following successful break-in, the perfusing medium was switched to an external recording solution containing (mM): N-methyl-D-glucamine aspartate (NMG-Asp), 137; Glucose, 10; Hepes, 10; $CaCl_2$, 1.8; $MgCl_2$, 0.5; CsCl, 25 (pH 7.4, adjusted with NMG). Signals were filtered at 2 kHz. Data traces were acquired at a repetition interval of 2 s from −70 to +60 at −80 mV holding potential. To determine the contribution of L- and T-type currents into common Ca^{2+} current we applied standard I/V protocols started from −80 mV (at −80 mV holding potential) and from −40 mV (at −40 mV holding potential) for T- and L-types correspondingly. We held the potential at −40 mV to inactivate T-type of Ca^{2+} current and then looked for any remaining transient inward current to 0 mV, near the peak of the L-type Ca^{2+}-current/voltage relationship.

Spontaneous action potentials of SAN cells were recorded under perforated-patch conditions by using amphotericin at 35 ± 1°C. SAN cells were identified by their morphology and spontaneous activity. The extracellular Tyrode solution contained (mM): NaCl, 140; KCl, 5.4; $CaCl_2$, 1.8; $MgCl_2$, 1.0; Hepes-NaOH, 5.0; and D-glucose, 5.5 (pH 7.4, adjusted with NaOH). The composition of the pipette solution was (mM): K aspartate, 130; NaCl, 10; ATP-Mg^{2+} salt, 2.0; creatine phosphate, 7.0; GTP-Na^+ salt, 0.1; $CaCl_2$, 0.04; and Hepes-KOH, 10 (pH 7.2, adjusted with KOH). Amphotericin (Sigma) was added to the pipette solution at a final concentration of 200 μg/ml.

RNA Preparation. Under general anesthesia with etomidate (30 mg/kg i.p.), mice were killed by cervical dislocation and the beating hearts were quickly excised. A thin strip of SAN tissue (≈1 × 0.8 mm), limited by the crista terminalis, the atrial septum, and the orifices of the venae cavae, was cut from the right atrium as previously described (5) and flash frozen in liquid nitrogen for further RNA isolation. Total RNA from pools of two SANs were isolated and DNase treated by using the RNeasy Fibrous Tissue Micro Kit (Qiagen) following manufacturer's instructions. The quality of total RNA was assessed by polyacrylamide gel microelectrophoresis (Agilent 2100 Bioanalyzer). Genomic DNA contamination was assessed by PCR amplification of total RNA samples without prior cDNA synthesis and no genomic DNA was detected.

TaqMan Quantitative RT-PCR. TaqMan Low Density Arrays (TLDA, Applied Biosystems) were completed in a two-step RT-PCR process as described previously (5). Briefly, first strand cDNA was synthesized from 200 ng of total RNA by using the High-Capacity cDNA Archive Kit (Applied Biosystems). PCRs were carried out in TLDA by using the ABI PRISM 7900HT Sequence Detection System (Applied Biosystems). The 384 wells of each array were preloaded with 96 × 4 predesigned FAM-labeled fluorgenic TaqMan probes and primers. The probes were labeled with the fluorescent reporter dye 6-carboxyfluorescein (FAM, Applera Corporation) on the 5′ end and with a nonfluorescent quencher on the 3′ end. The genes selected for analysis were ones encoding 67 ion channel pore-forming (α) and accessory (β) subunit proteins as well as proteins involved in ion channel regulation, nine proteins involved in calcium homeostasis, four transcription factors, specific markers of cardiac areas, vessels, neuronal tissue, fibroblasts, inflammation and hypertrophy, and four endogenous control genes used for normalization. The genes assayed are listed in Table S3. Two ng of cDNA from each sample was combined with 1X TaqMan Universal Master Mix (Applied Biosystems) and loaded into each well. The TLDA

were thermal-cycled at 50°C for 2 min and 94.5°C for 10 min, followed by 40 cycles of 97°C for 30 s and 59.7°C for 1 min. Data were collected with instrument spectral compensations by using the Applied Biosystems SDS 2.2.1 software and analyzed by using the comparative threshold cycle (C_T) relative quantification method. The *GAPDH* gene was used as an endogenous control to normalize the data. Genes with C_T values >30 were eliminated for lack of detection or reproducibility. Results in WT and transgenic animals are expressed as relative mRNA expression level as compared with *GAPDH*. Values are means ±SEM from two pools of two SANs in each group. Statistical analysis was performed by using the Student's *t* test.

1. Mohler PJ, *et al.* (2003) Ankyrin-B mutation causes type 4 long-QT cardiac arrhythmia and sudden cardiac death. *Nature* 421:634–639.
2. DiFrancesco D (1986) Characterization of single pacemaker channels in cardiac sino-atrial node cells. *Nature* 324:470–473.
3. Mangoni ME, Nargeot J (2001) Properties of the hyperpolarization-activated current (I_f) in isolated mouse sino-atrial cells. *Cardiovasc Res* 52(1):51–64.
4. World Medical Association (1997) World Medical Association Declaration of Helsinki: Recommendations guiding physicians in biomedical research involving human subjects. *Cardiovasc Res* 35(1):2–3.
5. Marionneau C, *et al.* (2005) Specific pattern of ionic channel gene expression associated with pacemaker activity in the mouse heart. *J Physiol* 562:223–234.
6. Wei SK, *et al.* (2007) Muscarinic modulation of the sodium-calcium exchanger in heart failure. *Circulation* 115:1225–1233.

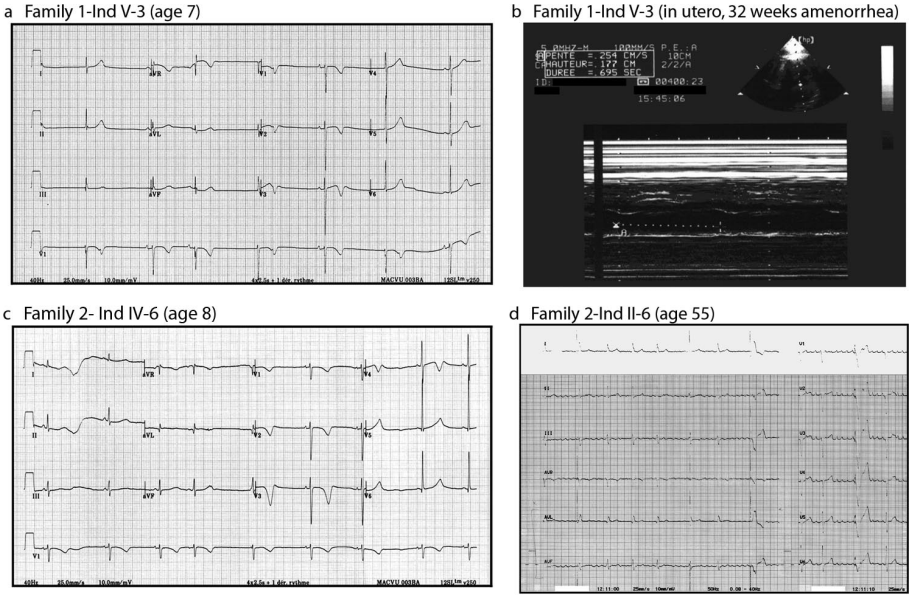

Fig. S1. SND in carriers of human ANK2 allele variants. (*a*) Family 1. ECG of patient V-3 recorded at 7 years showing severe sinus node dysfunction with a junctional escaped rhythm (heart rate 42 bpm) QT interval prolongation and T wave inversion. (*b*) Ultrasound recording of a human fetus (family 1, patient V3) revealing significant bradycardia with a heart rate of 86.3 bpm (compared to 125–160 bpm). (*c*) Family 2. ECG from patient IV-6 at 8 year showing severe sinus node dysfunction (heart rate 50 bpm), QT interval prolongation, and T wave inversion. (*d*) ECG showing an atrial fibrillation in patient II-6 (family 2) at 55 years-old, implanted with a pacemaker for sinus node dysfunction.

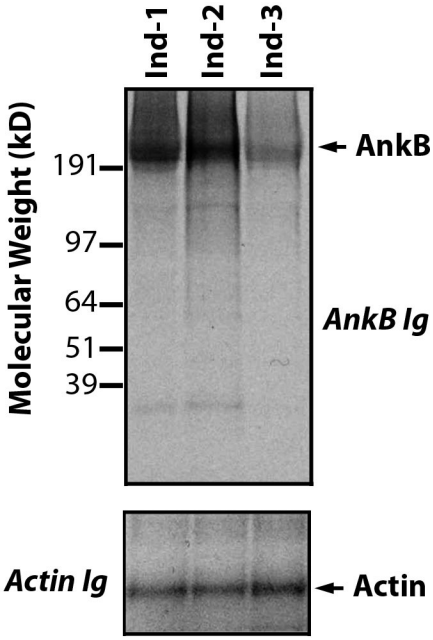

Fig. S2. Decreased ankyrin-B expression in human with mutant *ANK2* allele. Immunoblot of 50 micrograms of whole tissue lysate from pectoral muscle of two control individuals and patient with a mutant *ANK2* allele. Note the significant decrease in 220-kDa ankyrin-B expression in the individual with a mutant *ANK2* allele. Actin was used as a marker for equal loading.

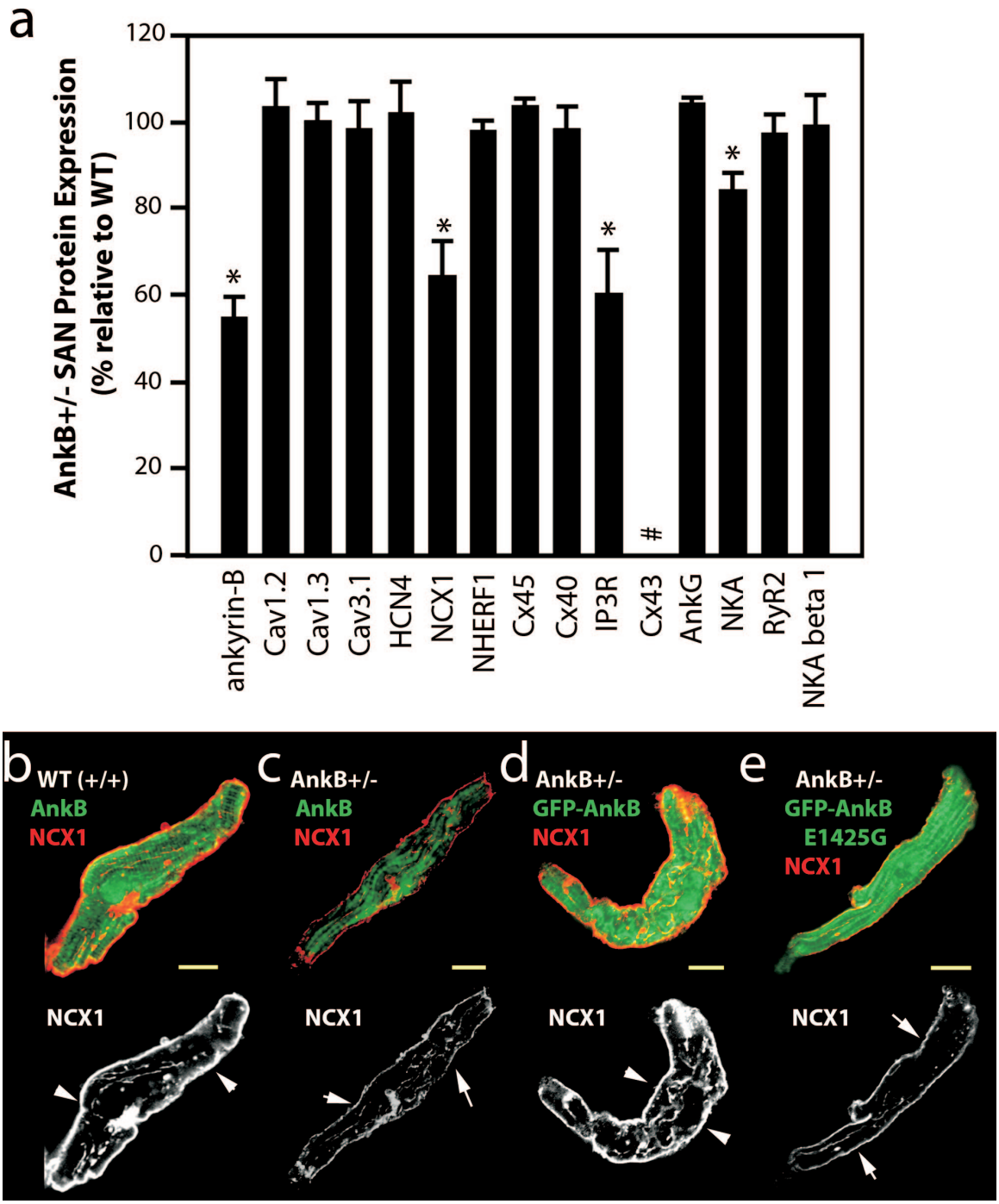

Fig. S3. NCX1, IP3R, and Na/K ATPase expression is affected in AnkB$^{+/-}$ SAN cells. (*a*) Reduced NCX1, IP3R, and Na/K ATPase protein levels in AnkB$^{+/-}$ SAN as assessed by immunoblot. No difference in expression of other SAN proteins was observed in AnkB$^{+/--}$ SAN preparations. Graph represents immunoblot data from three pooled samples of SAN (three SAN per pool) and normalized for WT SAN protein levels ($P < 0.05$). We were unable to detect Cx43 expression in central SAN tissue samples (#). (*b*–*e*) Viral expression of AnkB rescues NCX1 expression to normal in AnkB$^{+/-}$ SAN myocytes. Expression of AnkB and NCX1 in WT (*b*) and AnkB$^{+/--}$ SAN myocytes (*c*). Note decreased NCX1 membrane staining (white arrows) in AnkB$^{+/-}$ SAN myocytes. (*d*) Lentiviral expression of GFP-AnkB restores to normal the membrane expression of NCX1 in AnkB$^{+/-}$ SAN myocytes. (*e*) Human AnkB E1425G is a loss-of-function variant in SAN. Although normally expressed and localized as endogenous AnkB, GFP-AnkB E1425G does not rescue aberrant NCX1 membrane expression phenotype in AnkB$^{+/-}$ SAN myocytes. (Scale bar for all panels, 20 μm.)

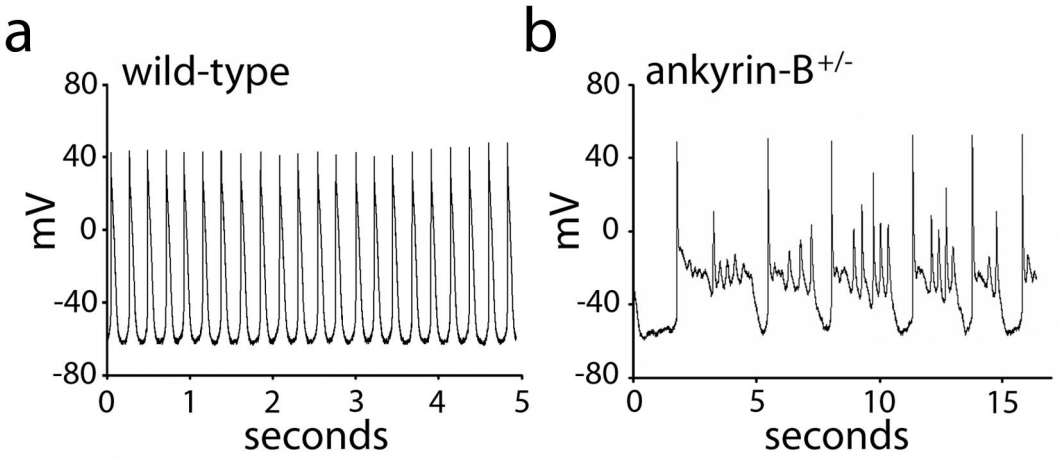

Fig. S4. AnkB$^{+/-}$ SAN cells display abnormal electrical activity. Action potentials recorded from single isolated SAN myocytes of WT and AnkB$^{+/-}$ mice. In addition to increased action potential cycle length, we observed after-depolarizations in SAN myocytes from a significant number of AnkB$^{+/-}$ mice (≈18%) versus WT mice (3%).

Table S1. Clinical characteristics of the *ANK2* mutation carriers of family 1 (AnkB-E1425G mutation)

No.	Current age	Pacemaker (age at implant)	Atrial fibrillation (age at diagnosis)	Patient age (ECG year)	HR (bpm)	Sinus node dysfunction	QT (ms)	QTc (ms)	QTU (ms)	Repolarization	Symptoms
II-2*	at 75†	No		70 (1975)	55	Yes (CSR)‡	480 (LBBB)	460 (LBBB)	—	Normal	
III-3	79	Yes (64)	Paroxysmal (58), perm. (60)	60 (1988)	52	Yes (CSR)	360	335	600	Sinusoidal TU wave	Palpitations, presyncope
III-5	77	Yes (57)	Permanent (72)	40 (1970)	50	Yes (JER)	460	420	600	Sinusoidal TU wave	Syncope
III-9	74	No	Permanent (63)	37 (1970)	45	Yes (JER)	530	460	810	Sinusoidal TU wave	Palpitations
III-15	70	Yes (56)	Paroxysmal (56)	53 (1990)	50	Yes (JER)	460	420	740	Sinusoidal TU wave	Palpitations
III-17	68	Yes (41)	Paroxysmal (41)	53 (1992)	45	Yes	400	346	700	Sinusoidal TU wave	Palpitations, syncope
III-19	65	Yes (49)	Paroxysmal (48), perm (59)	48 (1990)	40	Yes	460	376	680	Sinusoidal TU wave	Palpitations, syncope
III-21	64	No	Paroxysmal (23), perm (28)	34 (1977), AF	88	Yes	400	484	520	Normal	Palpitations
IV-5	51	No	Permanent (42)	36 (1992)	48	Yes (JER)	435	389	675	Sinusoidal TU wave	Palpitations
IV-7	48	Yes (34)		34 (1993)	63	Yes (JER)	380	389	560	Sinusoidal TU wave	
IV-8	46	Yes (31)	Paroxysmal (31)	31 (1992)	54	Yes (JER)	465	440	685	Sinusoidal TU wave	Palpitations
IV-10	39	No		29 (1997)	42	Yes (CSR)	440	368	600	Sinusoidal TU wave	
IV-12	36	No		23 (1994)	55	No	440	421	640	Sinusoidal TU wave	
IV-17	43	Yes (27)	Paroxysmal (27)	11 (1975)	55	Yes	440	421	600	Sinusoidal TU wave	Palpitations, presyncope
IV-19	42	Yes (23)	Paroxysmal (23)	23 (1988)	52	Yes (CSR)	440	410	600	Sinusoidal TU wave	Palpitations, presyncope
IV-26*	at 12†	No		11 (1973)	52	Yes (JER)	420	391	600	Sinusoidal TU wave	SD at 12 (exercise)
IV-28	38	No	Permanent (21)	10 (1979)	50	Yes (JER)	520	475	900	Sinusoidal TU wave	Palpitations
IV-31	34	Yes (22)		22 (1995)	41	Yes	400	331	560	Sinusoidal TU wave	Palpitations
IV-32	39	Yes (24)		9 (1977)	48	Yes (JER)	400	358	540	Sinusoidal TU wave	
IV-33	33	Yes (18)		33 (2007)	45	Yes (JER)	440	381	680	Sinusoidal TU wave	Palpitations, presyncope
IV-34	at 18†	Yes (16)	Paroxysmal (14), permanent (16)	11 (1982)	50	Yes (JER)	440	402	480	Sinusoidal TU wave	Palpitations, syncope, SD at 18 (being awakened)
IV-35	35	No		10 (1982)	84	Yes (CSR)	360	426	480	Sinusoidal TU wave	Palpitations
V-1	17	No		7 (1997)	68	Yes (CSR)	360	383		Normal	Syncope
V-3§	11	Yes (8)		7 (2003)	42	Yes (JER)	480	402	600	Sinusoidal TU wave	Presyncope
V-4	6	No		at birth (2001)	82	Yes	400	468	480	Sinusoidal TU wave	
V-9	8	No		at birth (1999)	90	Yes (CSR)	320	392	400	Sinusoidal TU wave	

*Unsequenced affected patients.
†Age at death.
‡AF, atrial fibrillation; CSR, coronary sinus rhythm; HR, heart rate; JER, junctional escape rhythm; LBBB, left bundle branch block; SD, sudden death.
§ECG is shown in Fig. S1.

Table S2. Clinical characteristics of the *ANK2* mutation carriers of family 2 (*ANK2* disease haplotype)

No.	Current age	Pace-maker (age at implant)	AF* (age at diagnosis)	Patient age (ECG year)	HR bpm	Sinus node dysfunction	QT (ms)	QTc (ms)	QTU (ms)	Repolarization	Symptoms
II-1	64	No	Paroxysmal (58)	59 (2002)	60	No	380	380	520	Normal	
II-6†	60	Yes (51)	Paroxysmal (50), perm (52)	55T(2002), AF	71	Yes	320	348	—	Normal	
II-7	58	No		53 (2002)	61	No	380	383	600	Sinusoidal TU wave	
II-9	55	No		50 (2002)	65	No	420	437	520	Normal	
II-11	51	No		46 (2002)	66	No	380	399	560	Normal	
III-1	43	Yes (43)		43 (2007)	33	Yes	520	386	700	Normal	Syncope
III-3	42	No		37 (2002)	60	No	380	380	—	Normal	
III-4	37	Yes (8)		32 (2002)	38	Yes	400	318	440	Sinusoidal TU wave	
III-9	42	Yes (40)		37 (2002)	41	Yes	440	364	480	Sinusoidal TU wave	Asthenia
III-12	38	Yes (29)	paroxysmal (35)	33 (2002)	48	Yes	420	376	560	Normal	Asthenia
III-13	36	No		31 (2002)	75	No	370	414	540	Sinusoidal TU wave	
III-17	33	No		28 (2002)	61	Yes (CSR)	370	373	600	Sinusoidal TU wave	Syncope
III-18	29	No		24 (2002)	49	Yes	440	398	560	Sinusoidal TU wave	Presyncope
III-19	24	No		19 (2002)	50	Yes (CSR)	440	402	600	Sinusoidal TU wave	
IV-1	10	No		10 (2007)	92	No	350	433	-	Normal	
IV-5	21	No		16 (2002)	49	Yes	360	325	560	Sinusoidal TU wave	
IV-6†	10	Yes (8)		8 (2005)	50	Yes	500	456	620	Sinusoidal TU wave	Asthenia
IV-7	9	No		5 (2003)	63	Yes	400	410	500	Sinusoidal TU wave	
IV-10	15	No		10 (2002)	56	Yes	400	386	560	Sinusoidal TU wave	
IV-12	8	No		8 (2007)	44	Yes (CSR)	460	394	560	Sinusoidal TU wave	
II-1	64	No	Paroxysmal (58)	59 (2002)	60	No	380	380	520	Normal	
II-6†	60	Yes (51)	Paroxysmal (50), perm (52)	55 (2002), AF	71	Yes	320	348	—	Normal	
II-7	58	No		53 (2002)	61	No	380	383	600	Sinusoidal TU wave	
II-9	55	No		50 (2002)	65	No	420	437	520	Normal	
II-11	51	No		46 (2002)	66	No	380	399	560	Normal	
III-1	43	Yes (43)		43 (2007)	33	Yes	520	386	700	Normal	Syncope

*AF, atrial fibrillation; CSR, coronary sinus rhythm; HR, heart rate.
†ECG is shown in Fig. S1.

Table S3. SAN genes analyzed by Taqman low density arrays

Gene symbol	Protein	NCBI gene ref	Chrom	Assay ID	Target exons
Abcc8	SUR1	NM_011510	7	Mm00803450_m1	19
Abcc9	SUR2	NM_011511	6	Mm00441638_m1	31
Actc1	cardiac α actin	NM_009608	2	Mm00477277_g1	2
Ank2	Ankyrin B	NM_178655	3	Mm00618325_m1	17
Atp1a1	α1 Na/K-ATPase	NM_144900	3	Mm00523255_m1	10
Atp1a2	α2 Na/K-ATPase	NM_178405	1	Mm00617899_m1	20
Atp1b1	β1 Na/K-ATPase	NM_009721	1	Mm00437612_m1	2
Atp2a2	SERCA2a	NM_009722	5	Mm00437634_m1	20
Cacna1c	Cav1.2	NM_009781	6	Mm00437917_m1	8
Cacna1d	Cav1.3	NM_028981	14	Mm00551384_m1	29
Cacna1 g	Cav3.1	NM_009783	11	Mm00486549_m1	9
Cacna1 h	Cav3.2	NM_021415	17	Mm00445369_m1	15
Cacna2d1	Cavα2δ1	NM_009784	5	Mm00486607_m1	33
Cacna2d2	Cavα2 δ 2	NM_020263	9	Mm00457825_m1	3
Cacna2d3	Cavα2 δ3	NM_009785	14	Mm00486613_m1	3
Cacnb1	Cavβ1	NM_031173	11	Mm00518940_m1	1
Cacnb2	Cavβ2	NM_023116	2	Mm00659092_m1	12
Cacnb3	Cavβ3	NM_007581	15	Mm00432233_m1	1
Cacng7	Cav δ7	NM_133189	7	Mm00519216_m1	1
Calm1	Calm1	NM_009790	12	Mm00486655_m1	2
Clcn2	ClC-2	NM_009900	16	Mm00438245_m1	22
Clcn3	ClC-3	NM_173876	8	Mm00432566_m1	4
Cnn1	Calponin 1	NM_009922	9	Mm00487032_m1	1
Col1a1	a1 Procollagen 1	NM_007742	11	Mm00801666_g1	49
Gja1	Cx43	NM_010288	10	Mm00439105_m1	1
Gja4	Cx37	NM_008120	4	Mm00433610_s1	8
Gja5	Cx40	NM_008121	3	Mm00433619_s1	6
Hcn1	Hcn1	NM_010408	13	Mm00468832_m1	3
Hcn2	Hcn2	NM_008226	10	Mm00468538_m1	3
Itpr2	IP3R-2	NM_019923	6	Mm00444937_m1	4
Kcna1	Kv1.1	NM_010595	6	Mm00439977_s1	1
Kcna2	Kv1.2	NM_008417	3	Mm00434584_s1	2
Kcna4	Kv1.4	NM_021275	2	Mm00445241_s1	4
Kcna5	Kv1.5	NM_145983	6	Mm00524346_s1	19
Kcna6	Kv1.6	NM_013568	6	Mm00496625_s1	14
Kcnb1	Kv2.1	NM_008420	2	Mm00492791_m1	1
Kcnd2	Kv4.2	NM_019697	6	Mm00498065_m1	4
Kcnd3	Kv4.3	NM_019931	3	Mm00498260_m1	4
Kcnh2	mERG	NM_013569	5	Mm00465370_m1	1
Kcnip2	KChIP2	NM_030716	19	Mm00518914_m1	1
Kcnj11	Kir6.2	NM_010602	7	Mm00440050_s1	13
Kcnj12	Kir2.2	NM_010603	11	Mm00440058_s1	6
Kcnj2	Kir2.1	NM_008425	11	Mm00434616_m1	1
Kcnj3	Kir3.1	NM_008426	2	Mm00434618_m1	2
Kcnj8	Kir6.1	NM_008428	6	Mm00434620_m1	2
Kcnk3	TASK	NM_010608	5	Mm00807036_m1	1
Kcnn1	SK1	NM_032397	8	Mm00446259_m1	4
Kcnn2	SK2	NM_080465	18	Mm00446514_m1	7
Kcnn3	SK3	NM_080466	3	Mm00446516_m1	2
Kcnq1	KvLQT1	NM_008434	7	Mm00434641_m1	11
Myh7	b MHC	NM_080728	14	Mm00600555_m1	39
Myl2	MLC2V	NM_010861	5	Mm00440384_m1	4
Myl4	MLC1A	NM_010858	11	Mm00440378_m1	2
Nedd4l	Nedd4–2	NM_031881	18	Mm00459584_m1	18
Nkx2–5	Nkx2.5	NM_008700	17	Mm00657783_m1	1
Nppb	BNP	NM_008726	4	Mm00435304_g1	1
Pias3	KchAP	NM_146135	3	Mm00450739_m1	5
Pln	PLB	NM_023129	10	Mm00452263_m1	1
Ryr2	RYR2	NM_023868	13	Mm00465877_m1	59
Scn1b	Navβ1	NM_011322	7	Mm00441210_m1	3
Scn4a	Nav1.4	NM_133199	11	Mm00500103_m1	10
Scn5a	Nav1.5	NM_021544	9	Mm00451971_m1	11
Scn7a	Nav2.1	NM_009135	2	Mm00801952_m1	24
Slc8a1	NCX1	NM_011406	17	Mm00441524_m1	9
Tbx2	T-box 2	NM_009324	11	Mm00436915_m1	6

Table S4. Post-transcriptional loss of expression of multiple ion channels/transporters in AnkB$^{+/-}$ SAN

Gene symbol	Protein	Gene name	het vs wt (% difference)
Abcc8	SUR1	ATP-binding cassette, sub-family C (CFTR/MRP), member 8	−11.67
Abcc9	SUR2	ATP-binding cassette, sub-family C (CFTR/MRP), member 9	−10.82
Actc1	cardiac α actin	Actin, alpha, cardiac	4.87
Ank2	Ankyrin B	Ankyrin 2, brain	−31.25
Atp1a1	α1 Na/K-ATPase	ATPase, Na^+/K^+ transporting, alpha 1 polypeptide	10.05
Atp1a2	α2 Na/K-ATPase	ATPase, Na^+/K^+ transporting, alpha 2 polypeptide	17.89
Atp1b1	β1 Na/K-ATPase	ATPase, Na^+/K^+ transporting, beta 1 polypeptide	6.08
Atp2a2	SERCA2a	ATPase, Ca^{2+} transporting, cardiac muscle, slow twitch 2	12.23
Cacna1c	Cav1.2	Calcium channel, voltage-dependent, L type, alpha 1C subunit	6.41
Cacna1d	Cav1.3	Calcium channel, voltage-dependent, L type, alpha 1D subunit	6.55
Cacna1 g	Cav3.1	Calcium channel, voltage-dependent, T type, alpha 1G subunit	6.66
Cacna1 h	Cav3.2	Calcium channel, voltage-dependent, T type, alpha 1H subunit	12.32
Cacna2d1	Cavα2 δ1	Calcium channel, voltage-dependent, alpha2/delta subunit 1	4.16
Cacna2d2	Cavα2 δ2	Calcium channel, voltage-dependent, alpha 2/delta subunit 2	8.61
Cacna2d3	Cavα2δ3	Calcium channel, voltage dependent, alpha2/delta subunit 3	22.75
Cacnb1	Cav β1	Calcium channel, voltage-dependent, beta 1 subunit	−11.63
Cacnb2	Cav β2	Calcium channel, voltage-dependent, beta 2 subunit	−10.49
Cacnb3	Cav β3	Calcium channel, voltage-dependent, beta 3 subunit	−16.25
Cacng7	Cav δ7	Calcium channel, voltage-dependent, gamma subunit 7	15.21
Calm1	Calm1	Calmodulin 1	−4.98
Clcn2	ClC-2	Chloride channel 2	−2.97
Clcn3	ClC-3	Chloride channel 3	11.62
Cnn1	Calponin 1	Calponin 1	−2.59
Col1a1	α1 Procoll- 1	Procollagen, type I, alpha 1	5.50
Gja1	Cx43	Gap junction membrane channel protein alpha 1	−9.59
Gja4	Cx37	Gap junction membrane channel protein alpha 4	3.89
Gja5	Cx40	Gap junction membrane channel protein alpha 5	0.47
Hcn1	Hcn1	Hyperpolarization-activated, cyclic nucleotide-gated K^+ 1	−14.68
Hcn2	Hcn2	Hyperpolarization-activated, cyclic nucleotide-gated K^+ 2	23.77
Itpr2	IP3R-2	Inositol 1,4,5-triphosphate receptor 2	0.70
Kcna1	Kv1.1	Voltage-gated K channel, shaker-related subfamily, member 1	21.50
Kcna2	Kv1.2	Voltage-gated K channel, shaker-related subfamily, member 2	26.16
Kcna4	Kv1.4	Voltage-gated K channel, shaker-related subfamily, member 4	−13.81
Kcna5	Kv1.5	Voltage-gated K channel, shaker-related subfamily, member 5	−3.28
Kcna6	Kv1.6	Voltage-gated K channel, shaker-related, subfamily, member 6	−5.79
Kcnb1	Kv2.1	Voltage gated K channel, Shab-related subfamily, member 1	1.24
Kcnd2	Kv4.2	Voltage-gated K channel, Shal-related family, member 2	2.71
Kcnd3	Kv4.3	Voltage-gated K channel, Shal-related family, member 3	24.94
Kcnh2	mERG	Voltage-gated K channel, subfamily H (eag-related), member 2	−7.64
Kcnip2	KChIP2	Kv channel-interacting protein 2	−3.44
Kcnj11	Kir6.2	Potassium inwardly rectifying channel, subfamily J, member 11	2.76
Kcnj12	Kir2.2	Potassium inwardly-rectifying channel, subfamily J, member 12	7.29
Kcnj2	Kir2.1	Potassium inwardly-rectifying channel, subfamily J, member 2	8.94
Kcnj3	Kir3.1	Potassium inwardly-rectifying channel, subfamily J, member 3	18.34
Kcnj8	Kir6.1	Potassium inwardly-rectifying channel, subfamily J, member 8	2.60
Kcnk3	TASK	Potassium channel, subfamily K, member 3	−13.36
Kcnn1	SK1	Ca-activated K channel, subfamily N, member 1	6.60
Kcnn2	SK2	Ca-activated K channel, subfamily N, member 2	−11.05
Kcnn3	SK3	Ca-activated K channel, subfamily N, member 3	31.12
Kcnq1	KvLQT1	Potassium voltage-gated channel, subfamily Q, member 1	−5.58
Myh7	β MHC	Myosin, heavy polypeptide 7, cardiac muscle, beta	4.60
Myl2	MLC2V	Myosin, light polypeptide 2, regulatory, cardiac, slow	20.67
Myl4	MLC1A	Myosin, light polypeptide 4	−11.31
Nedd4l	Nedd4–2	Neural precursor cell expressed, dev down-regulated gene 4-like	−2.50
Nkx2–5	Nkx2.5	NK2 transcription factor related, locus 5 (Drosophila)	−8.59
Nppb	BNP	Natriuretic peptide precursor type B	−46.38
Pias3	KChAP	Protein inhibitor of activated STAT 3	−0.21
Pln	PLB	Phospholamban	0.79
Ryr2	RYR2	Ryanodine receptor 2, cardiac	5.65
Scn1b	Navβ1	Sodium channel, voltage-gated, type I, beta polypeptide	−7.10
Scn4a	Nav1.4	Sodium channel, voltage-gated, type IV, alpha polypeptide	−10.16
Scn5a	Nav1.5	Sodium channel, voltage-gated, type V, alpha polypeptide	−13.04
Scn7a	Nav2.1	Sodium channel, voltage-gated, type VI, alpha polypeptide	3.22
Slc8a1	NCX1	Solute carrier family 8 (sodium/calcium exchanger), member 1	25.33

Gene symbol	Protein	Gene name	het vs wt (% difference)
Tbx2	T-box 2	T-box 2	2.72
Tbx3	T-box 3	T-box 3	28.64
Tbx5	T-box 5	T-box 5	−4.06
Tnni1	sk troponin I	Troponin I, skeletal, slow 1	35.60
Tnni3	card troponin I	Troponin I, cardiac	24.29
Uchl1	UCHL1	Ubiquitin carboxy-terminal hydrolase L1	−3.22

TaqMan Low Density Array on pools of sinoatrial nodes isolated from WT and AnkB$^{+/-}$ mice reveal no significant change in mRNA levels of major cardiac mRNAs (see Table S3 for specific details on mRNAs tested).